in hand can such an assignment be safely made.

An interesting feature of the Mn(SALPS) unit is the Mn(II)–disulfide bond. As shown in Scheme I, an Mn(II)–disulfide lies at one extreme of an internal electron-transfer network. An Mn(IV)–dithiolate can be formulated at the other end of the system. That Mn(SALPS) lies at the extreme left of this diagram is supported by the following observations: (1) the S1–S2 bond length is typical of a coordinated disulfide; (2) while S2 is in bonding distance of the Mn, S1 is nearly 4 Å from the Mn atom; (3) the magnetic data are consistent with a high-spin Mn(II) formulation (μ = 5.94 μ_B). This result is not surprising as Mn(IV) is a strongly oxidizing species and would be expected to undergo redox reactions with thiolate sulfur atoms; however, the notion that the disulfide functional group may act as a two-electron sink for the internal transformation of oxidation states in a given complex represents a fertile area for future studies. In this regard, we are presently investigating the preparation of Mn(I)–disulfides as precursors to Mn(III)–dithiolates.

Acknowledgment. We wish to thank Professor J. L. Dye for the use of the SQUID susceptometer and Joe Skywora and Ira Finkelstein for experimental assistance. We also wish to thank Professors D. Coucouvanis, P. Rasmussen, and A. Francis for enlightening discussions. This work was supported by the donors of the Petroleum Research Fund, administered by the American Chemical Society, and the Horace H. Rackham Foundation.

Supplementary Material Available: Table VII, fractional atomic coordinates for hydrogen atoms of Mn(SALPS)CH_3OH·CH_3OH, Table VIII, thermal parameters for Mn(SALPS)CH_3OH·CH_3OH, Table IX, bond distances for Mn(SALPS)CH_3OH·CH_3OH, Table X, bond angles for Mn(SALPS)CH_3OH·CH_3OH, Table XII, thermal parameters for $[Mn(SALPS)]_2$·$2CH_3CN$, Table XIII, bond distances for $[Mn(SALPS)]_2$·$2CH_3CN$, Table XIV, bond angles for $[Mn(SALPS)]_2$·$2CH_3CN$, Table XVI, χ_m values for $[Mn(SALPS)]_2$, Table XVII, μ_{eff} for $[Mn(SALPS)]_2$, and Table XVIII, fractional atomic coordinates for hydrogen atoms of $[Mn(SALPS)]_2$·$2CH_3CN$, and Figure 8, numbering scheme for Mn(SALPS)CH_3OH·CH_3OH, Figure 9, numbering scheme for $[Mn(SALPS)]_2$·$2CH_3CN$, Figure 10, stereoview of $[Mn(SALPS)]_2$, and Figure 11, packing diagrams for Mn(SALPS)CH_3OH·CH_3OH and $[Mn(SALPS)]_2$·$2CH_3CN$ (19 pages); Table XI, structure factors for Mn(SALPS)CH_3OH·CH_3OH, and Table XV, structure factors for $[Mn(SALPS)]_2$·$2CH_3CN$ (27 pages). Ordering information is given on any current masthead page.

Contribution from the Inorganic Chemistry Laboratory, ETH-Zentrum, CH-8092 Zürich, Switzerland, and Department of Chemistry, Politecnico di Milano, I-20133 Milan, Italy

Preparative and ^{1}H NMR Spectroscopic Studies on Palladium(II) and Platinum(II) Quinoline-8-carbaldehyde (1) Complexes. X-ray Structures of the Cyclometalated Acyl Complex $\overline{PdCl(C(O)C_9H_6N)}(PPh_3)$·$PPh_3$ and *trans*-$PtCl_2(1)(PEt_3)$

A. Albinati,*‡ C. G. Anklin,† F. Ganazzoli,‡ H. Rüegg,† and P. S. Pregosin*†

Received July 22, 1986

A series of complexes of the type *trans*-$PtCl_2$(quinoline-8-carbaldehyde)L (**2**; L = PEt_3, $PTol_3$ (Tol = *p*-$CH_3C_6H_4$), PPh_3, $AsMe_3$, $AsEt_3$, As-*i*-Pr_3, As-*n*-Bu_3, $AsTol_3$, $AsMePh_2$) have been synthesized and characterized. The aldehyde proton couples to ^{195}Pt with a value between 12.4 and 19.7 Hz. We interpret these NMR spectroscopic data as implying a weak Pt←H–C(O) interaction that is not of the previously reported agostic type. Complexes **2** cyclometalate at the aldehyde carbon in refluxing $CHCl_3$. The structure of an intermediate of type **2**, with L = PEt_3, has been determined. Complex **2a** has a square-planar trans geometry with the C–H vector of the aldehyde pointing toward the platinum and the aldehyde oxygen away from the metal center. The molecule is monoclinic, space group $P2_1/c$, with a = 14.411 (3) Å, b = 9.172 (2) Å, c = 15.217 (4) Å, β = 107.07 (2)°, V = 1929.5 Å^3, and Z = 4. The X-ray structure of the palladium acyl complex $\overline{PdCl(C(O)C_9H_6N)}(PPh_3)$·$PPh_3$ (**3**) is reported. The molecule has a square-planar coordination sphere with the acyl carbon trans to Cl and phosphorus trans to the quinoline nitrogen. A molecule of PPh_3 is trapped in the crystal lattice. The molecule crystallizes in the space group $P2_1/c$, with a = 10.159 (4) Å, b = 18.262 (5) Å, c = 21.171 (5) Å, β = 103.27 (3)°, and Z = 4. The long Pd–Cl bond separation of 2.421 (2) Å is in keeping with a large trans influence for the acyl function.

Introduction

Although the cyclometalation of aromatic, and to a lesser extent aliphatic, carbon atoms is widely recognized,[1,2] there is relatively little known concerned with the cyclometalation of aldehyde functions. We have shown that both 2-hydroxy-[3] and 2-(dimethylamino)benzaldehyde[4] can be made to cyclometalate at the aldehyde carbon by using Pd(II) and Pt(II) salts, and Landvatter and Rauchfuss[5] have shown a similar reaction with 2-(diphenylphosphino)benzaldehyde. In all three cases the coordination of either an oxygen, nitrogen, or phosphorus function precedes the cyclometalation. We have recently[6] explored similar chemistry starting from the Pd(II) and Pt(II) dimers $[MCl(\mu\text{-}Cl)l]_2$ plus quinoline-8-carbaldehyde (**1**) (see eq 1). Surprisingly, we have

$$^1/_2[PtCl(\mu\text{-}Cl)(PEt_3)]_2 + \mathbf{1} \rightarrow \mathbf{2} \xrightarrow{\Delta} \overline{PtCl(C(O)C_9H_6N)}(PEt_3) + HCl \quad (1)$$

observed a 13.7-Hz proton–platinum-195 coupling constant (I = $^1/_2$, natural abundance = 34%) between the metal and the aldehyde proton in complex **2a**, an intermediate leading to the acyl complex. The X-ray crystallography for **2a** (see below) clearly shows the C–H vector of the aldehyde to be situated favorably for an interaction with the platinum, so that our solution NMR

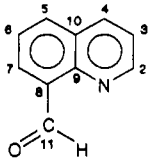

1

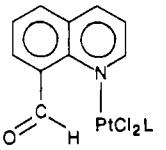

2

L = (a) PEt_3, (b) $PTol_3$, (c) PPh_3, (d) $AsMe_3$, (e) $AsEt_3$, (f) As-*i*-Pr_3, (g) As-*n*-Bu_3, (h) $AsTol_3$, (i) $AsMePh_2$

† ETH-Zentrum.
‡ Politecnico di Milano.

(1) Constable, E. C. *Polyhedron*, **1984**, *3*, 1037.
(2) Bruce, M. I. *Angew. Chem., Int. Ed. Engl.* **1977**, *16*, 73.
(3) Anklin, C.; Pregosin, P. S.; Bachechi, F.; Mura, P.; Zambonelli, L. *J. Organomet. Chem.* **1981**, *222*, 175. Motschi, H.; Pregosin, P. S.; Rüegger, H. *J. Organomet. Chem.* **1980**, *194*, 397.
(4) Anklin, C. G.; Pregosin, P. S. *J. Organomet. Chem.* **1983**, *243*, 101.
(5) Landvatter, E. F.; Rauchfuss, T. B. *Organometallics* **1982**, *193*, 506.
(6) Albinati, A.; Anklin, C. G.; Pregosin, P. S. *Inorg. Chim. Acta* **1984**, *90*, L37.

0020-1669/87/1326-0503$01.50/0

Table I. Analytical Data for the Complexes

L	formula	anal. % C calcd	% C found	% H calcd	% H found	% N calcd	% N found	% Cl calcd	% Cl found
				$PtCl_2(1)L$					
PEt_3	$C_{16}H_{22}Cl_2NOPPt$	35.49	35.56	4.13	4.21	2.59	2.64	13.09	13.39
PPh_3	$C_{28}H_{22}Cl_2NOPPt$	49.06	48.84	3.24	3.23	2.04	2.03	10.34	11.25
As-*n*-Bu_3	$C_{22}H_{34}AsCl_2NOPt$	39.47	39.43	5.12	5.17	2.09	2.03	10.59	10.55
$AsTol_3$	$C_{31}H_{28}AsCl_2NOPt$	48.26	48.45	3.66	3.72	1.82	1.68	9.19	9.25
$AsMePh_2$	$C_{23}H_{20}AsCl_2NOPt$	41.40	41.32	3.02	2.75	2.10	2.09	10.63	10.32
				$PtCl(C(O)C_9H_6N)L$					
PEt_3	$C_{16}H_{21}ClNOPPt$	38.06	38.13	4.19	4.20	2.77	2.90	7.02	7.10
As-*n*-Bu_3	$C_{22}H_{33}AsClNOPt$	41.75	41.73	5.25	5.25	2.21	2.07	5.60	5.63

measurement may correlate with the solid-state observation; moreover, a similar spin–spin coupling is also observed in related 8-substituted quinoline compounds, e.g., 8-methyl-, 8-isopropyl-, and 8-dibromoethylquinoline, all of which show J(Pt,H) values ranging from 12 to 39 Hz.[7] These NMR data suggest an interaction of the metal with H(11) that does not proceed through the quinoline bonds, but rather involves some form of three-center bonding. Consequently, these coupling constants are potentially of interest in that they may provide an indication of a developing interaction between the metal and the C–H bond. We report here an extension of these spectroscopic studies to include a wider variety of L ligands as well as the X-ray structures of (i) a cyclometalated palladium analogue $PdCl(C(O)C_9H_6N)(PPh_3)\cdot PPh_3$ (**3**), whose structure revealed one coordinated and one noncoordinated PPh_3 ligand, and (ii) the intermediate **2a**.

Results and Discussion

NMR Data. The derivatives of **2a–i** are readily prepared by treating the dimers $[PtCl(\mu\text{-}Cl)L]_2$[8] with 2 equiv of **1** in either chloroform or methylene chloride. The acyl complexes arise from **2** by refluxing in chloroform for several hours. The HCl that is released escapes at this temperature.[9] Analytical data for some representative complexes are given in Table I.

The ^{1}H NMR spectra for all of the complexes **2** show a coupling between the aldehyde proton H(11) and platinum-195, with values falling in the range 12.4–19.7 Hz. The aldehyde proton chemical shifts are all similar at δ 13.09–13.45, a low-field position relative to that of free **1**, δ = 11.48. Table II provides a compilation of these and other data. The proton H(2), immediately adjacent to nitrogen, represents the only other hydrogen for which we observe a coupling to the metal. Its values ^3J(Pt,H), 17.6–27.0 Hz, are reasonable[10] and vary qualitatively with the trans influence of L: i.e. alkylphosphine > arylphosphine; alkylarsine > arylarsine; alkylphosphine > alkylarsine. This is in keeping with what is known[11] for the trans influence in Pt(II) chemistry. In contrast with H(2), we do not feel that the trans influence of L can be readily correlated to J{Pt,H(11)} but do note that, for our series of arsines, this coupling constant tends to decrease with increasing size of the arsine ligand. Specifically, the L-dependent sequence for J{Pt,H(11)} is $AsMe_3$ > $AsMePh_2$ > $AsEt_3$ > As-*n*-Bu_3 > $AsTol_3$ > As-*i*-Pr_3, suggesting that as L increases in size the aldehyde proton adopts a slightly different position with respect to the metal.

^{13}C data for **2** were obtained in the hopes that both $\delta(^{13}C(11))$ and $^1J(^{13}C,^1H)$ would provide additional probes for changes at the aldehyde carbon. $\delta(^{13}C(11))$ does change slightly from 192.6 in **1** in 188.1 in **2a** and is accompanied by a J{^{195}Pt,^{13}C(11)} value of 31.6 Hz (J{^{31}P,^{13}C(11)} = 3.5 Hz); however, there is little or no change in the $^1J(^{13}C,^1H)$ values, which are 185 and 183 Hz, respectively. For complex **2d** $\delta(^{13}C(11))$ = 187.4 and $J(^{195}Pt,^{13}C)$ = 29.6 Hz. The presence of a relatively large J{^{195}Pt,^{13}C(11)} value is also suggestive of a coupling mechanism other than through the quinoline bonding framework; however, we feel that not enough is known about platinum–carbon coupling through four bonds to permit us to place emphasis on these data. We have also determined $^1J(^{13}C,^{13}C)$ values for **1**, **2a**, and the acylpalladium complex $PdCl(C(O)C_9H_6N)(PPh_3)$ in order to exclude major electronic changes in the carbon skeleton, and these data are shown in the Scheme I. Although the quinoline backbone shows slight variations when the three compounds are compared, ^1J{^{13}C(8),^{13}C(11)} remains unchanged at ca. 61 Hz. While this observation can be rationalized for **1** and **2a**, we were surprised that the cyclopalladated product showed almost no change, in view of the angular distortion involved in forming the five-membered ring.

Table II. ^{1}H NMR Data[a] for the Complexes $PtCl_2(1)L$

L	J{Pt,H(11)}, Hz	δ(H(11))	^3J{Pt,H(2)}, Hz	δ(H(2))
PEt_3	13.7	13.09	17.6	9.50
$PTol_3$	12.4	13.26	20.5	9.64
PPh_3	12.4	13.23	20.5	9.63
$AsMe_3$	19.7	13.12	24.6	9.50
$AsEt_3$	15.4	13.27	23.2	9.57
As-*i*-Pr_3	13.7	13.39	21.6	9.61
As-*n*-Bu_3	15.2	13.28	23.8	9.57
$AsTol_3$	14.7	13.45	27.0	9.69
$AsMePh_2$	17.4	13.32	26.7	9.60

[a] $CDCl_3$ solutions. Coupling constants are ±0.3 Hz; chemical shifts are 0.01 ppm. [b] Best measured by using a "low-field" spectrometer, i.e. 90 or 100 MHz for ^{1}H spectra.[7]

Scheme I. $^1J(^{13}C,^{13}C)$ Values in Hz for **1**, **2a**, and the Acylpalladium Complex[a]

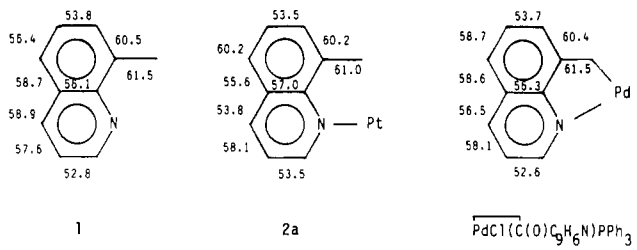

1 2a $PdCl(C(O)C_9H_6N)PPh_3$

[a] Coupling constants are placed between the appropriate carbons (oxygen not shown).

IR Data. We have also measured some IR spectra, with the view of determining changes in $\nu_{C=O}$ for **1** and **2a**. Both in $CHCl_3$ solution and as KBr pellets, we find $\nu_{C=O}$ values of ca. 1685 and 1681 cm^{-1}, respectively, suggesting little or no change in the carbonyl stretching frequency due to complexation. The corresponding value for the $AsEt_3$ compound was 1685 cm^{-1}. Interestingly, we find the C–H(11) stretch of **2a** at 2742 cm^{-1} (2080

(7) Anklin, C. G.; Pregosin, P. S. *Magn. Reson. Chem.* **1985**, *23*, 671.
(8) Smithies, A. C.; Schmidt, P.; Orchin, M. *Inorg. Synth.* **1970**, *12*, 240. Goodfellow, R. J.; Venanzi, L. M. *J. Chem. Soc.* **1965**, 7533.
(9) If the reaction is carried out at room temperature, 0.5 equiv of the quinoline functions as a base and produces the quinolinium chloride salt.
(10) Kaplan, P. D.; Schmidt, P.; Brause, A.; Orchin, M. *J. Am. Chem. Soc.* **1969**, *91*, 85. Marcelis, A. T. M.; van Kralingen, C. G.; Opschoor, S.; Reedijk, J. *Recl.: J. R. Neth. Chem. Soc.* **1980**, *99*, 198. Beyerle-Pfnur, R.; Jaworski, S.; Lippert, B.; Schöllhorn, H.; Thewalt, U. *Inorg. Chim. Acta* **1985**, *107*, 217.
(11) Motschi, H.; Pregosin, P. S. *Inorg. Chim. Acta* **1980**, *40*, 141. Motschi, H.; Pregosin, P. S.; Venanzi, L. M. *Helv. Chim. Acta* **1979**, *62*, 667.

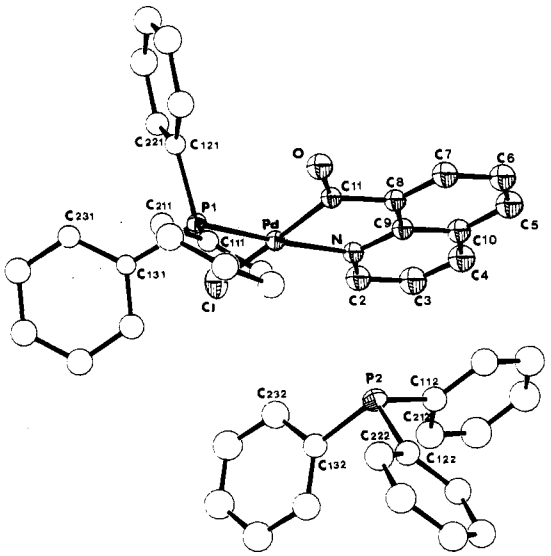

Figure 1. ORTEP view of the complex $PdCl(C(O)C_9H_6N)(PPh_3)\cdot PPh_3$. For clarity only the first two carbon atoms of the phenyl rings have been labeled: the first digit refers to the carbon atom number (1–6), the second to the phenyl ring (1–3) and the last to the number of the phosphorus atom to which the *ipso*-carbon is bound.

cm^{-1} for the C–D analogue), whereas for **1** this vibration appears at 2876 cm^{-1} (2163 cm^{-1} in the C–D compound). The decrease in energy for **2a** relative to **1** may stem from interaction with the metal, assuming pure vibrations.

Molecular Structures. (i) $PdCl(C(O)C_9H_6N)(PPh_3)$. The complexes **2** and their palladium counterparts convert smoothly to their cyclometalated derivatives at 60 °C in chloroform. The structure of the platinum derivatives can be deduced from ^1H, ^{13}C, and ^{31}P NMR studies in conjunction with IR and microanalytical data. The decision for a geometry in which L is trans to N can be made on the basis of $^1J(^{195}Pt,^{31}P)$.[12] For the palladium analogues of 2, however, this NMR tool is not available. Moreover, as there is considerable interest in the chemistry of 8-substituted quinolines,[13,14] we have determined the structure of the PPh_3 acyl complex $PdCl(C(O)C_9H_6N)(PPh_3)$.

The complex itself has the expected distorted-square-planar geometry as shown in Figure 1. The Cl(1) and O(1) atoms are displaced from the coordination plane (defined by the quinoline N, the Pd, and the P atoms) by about 0.24 Å. The phosphine is trans to the quinoline nitrogen, and the chloride opposite to the acyl carbon. A consequence of this latter orientation is the very long Pd–Cl bond length of 2.421 (2) Å. Some 10 years ago, Steffen and Palenik[15] compiled Pd–Cl bond distances as a function of the trans ligand and found a range of ca. 2.24–2.45 Å with σ-bound carbon atoms responsible for the high end of the range. More recently, Bardi et al.[16a] have reported a 2.430 (4) Å Pd–Cl distance in the complex *trans*-$PdCl(CO(n\text{-hex}))(PPh_3)_2$ (*n*-hex = *n*-hexyl). Given these data, we can confidently confirm our recent suggestion[17] of the large trans influence associated with the acyl function. The remaining bond separations are normal (see Table III), allowing for the appropriate trans influences; e.g., the Pd–P(1) separation of 2.267 (2) Å is slightly longer than that observed for PPh_3 trans to Cl[16b] but shorter than the 2.337 (1) Å found for *trans*-$PdCl_2(PPh_3)_2$.[18] Once again[17] we find the acyl

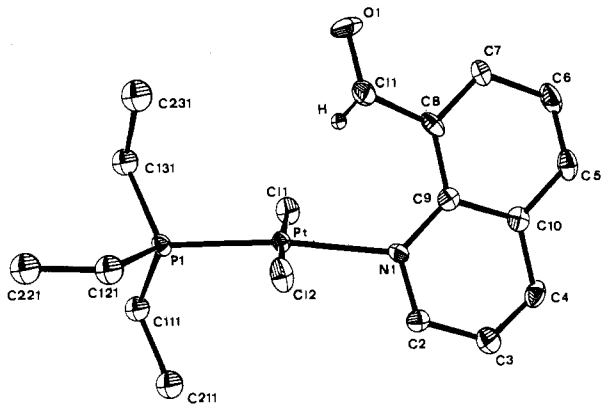

Figure 2. ORTEP view of **2a** with the numbering scheme.

carbon–metal separation, 1.981 (8) Å, interesting and short enough to be suggestive of back-bonding; however, the large uncertainty rules out anything but speculation. Typically, the Pt- and Pd–acyl carbon distances fall in the range 1.96–2.05 Å.[17] The bond angles about palladium are dictated by the five-membered ring, which at 83.1 (2)° is small enough to allow the large PPh_3 ligand to move slightly toward the carbonyl, thereby decreasing the P(1)–Pd–N angle, 173.1 (2)°, and increasing the P(1)–Pd–Cl angle, 96.3 (1)°, relative to 180 and 90°, respectively.

An unusual feature of the structure is the presence of a second PPh_3 ligand, uncoordinated, in the unit cell. This second phosphorus atom is more than 4 Å away from the palladium and for all intents and purposes may be considered a "free" ligand. A comparison of these two different PPh_3 molecules reveals no significant difference in the P(1)–C and P(2)–C distances (average value 1.83 (1) Å) and C–P–C angles (average values 104 ± 2 and 102 ± 1° for Pt(1) and P(2), respectively) apart from their conformations.[19-21]

(ii) 2a. A proper understanding of the NMR data required that we consider the possibility that the structure of **2**, and specifically **2a**, contained a coordinated aldehyde oxygen. That this is not the case in the solid state is shown in Figure 2, where we give a view of the structure of this molecule. The most obvious feature of the aldehyde function is that the carbon–oxygen vector faces away from the platinum, affording an oxygen–platinum separation of ca. 4 Å. Table III also shows a selection of bond lengths and bond angles for this molecule. A preliminary report of its structure has appeared.[6]

The local complex geometry is distorted square planar with trans chloride ligands. The Pt–Cl separations 2.286 (5) and 2.287 (5) Å, are normal[22,23] as are the Pt–P, 2.222 (4) Å, and Pt–N, 2.155 (13) Å, bond distances. With respect to the quinoline ring the only significant differences between compounds **2a** and **3** are due to the steric strain imposed by the formation of the cyclometalated ring, i.e. angles involving C(8), C(9), and N(1).

The quinoline moiety is approximately perpendicular to the plane, as judged by the torsion angles listed in Table III. This is reasonable for a sterically demanding pyridine,[24,25] and consequently the aldehyde group is positioned above the coordination plane. The C–H vector has been located and points toward the

(12) Kunz, R. W.; Pregosin, P. S. *NMR: Basic Princ. Prog.* **1979**, *16*.
(13) Suggs, J. W.; Wovkulich, M. J.; Cox, S. W.; Jun, C. *J. Am. Chem. Soc.* **1984**, *106*, 3054.
(14) Deeming, A. J.; Rothwell, I. P. *Pure Appl. Chem.* **1980**, *52*, 649 Deeming, A. J.; Rothwell, I. P.; Hursthouse, M. B.; New, L. *J. Chem. Soc., Dalton Trans.* **1978**, 1490.
(15) Steffen, W. L.; Palenik, G. J. *Inorg. Chem.* **1976**, *15*, 2432.
(16) Bardi, R.; Piazzesi, A. M.; Del Pra, A.; Cavinato, G.; Toniolo, L. *Inorg. Chim. Acta* **1985**, *102*, 99; **1983**, *75*, 15.
(17) Albinato, A.; von Gunten, U.; Pregosin, P. S.; Rüegg, H. J. *J. Organometa. Chem.* **1985**, *295*, 239.
(18) Ferguson, G.; McCrindle, R.; McAlees, A. J.; Parvez, M. *Acta Crystallogr., Sect. B: Struct. Crystallogr. Cryst. Chem.* **1982**, *B38*, 2679
(19) Brock, C. P.; Ibers, J. A. *Acta Crystallogr., Sect. B: Struct. Crystallogr. Cryst. Chem.* **1973**, *B29*, 2426.
(20) Daly, J. J. *J. Chem. Soc.* **1964**, 3799.
(21) (a) Bürgi, H. B.; Dunitz, J. D. *Acc. Chem. Res.* **1983**, *16*, 153. (b) Bye, H.; Bernd-Schweizer, W.; Dunitz, J. D. *J. Am. Chem. Soc.* **1982**, *104*, 5893.
(22) Albinati, A.; Moriyama, H.; Rüegger, H.; Pregosin, P. S.; Togni, A. *Inorg. Chem.* **1985**, *24*, 4430.
(23) Sin, G. A.; Sutton, L. E. *Molecular Structure by Diffraction Methods*; The Chemical Society: London, 1972; Vol. 1, p 606.
(24) Camalli, M.; Caruso, F.; Zambonelli, L. *Inorg. Chim. Acta* **1980**, *44*, L177.
(25) Rochon, F. D.; Kong, P. C.; Melanson, R. *Can. J. Chem.* **1980**, *58*, 97. Rochon, F. D.; Melanson, R. *Acta Crystallogr., Sect. B: Struct. Crystallogr. Cryst. Chem.* **1980**, *B36*, 691.

Table III. Selected Bond Lengths (Å), Angles (deg), and Torsion Angles (deg) for $\overline{PdCl(C(O)C_9H_6N)}\cdot PPh_3$ (**3**) and $PtCl_2(1)PEt_3$ (**2a**) (Esd's Given in Parentheses)

	3 (M = Pd)	**2a** (M = Pt)		**3** (M = Pd)	**2a** (M = Pt)
			Bond Lengths		
M-P(1)	2.267 (2)	2.222 (4)	C(6)-C(7)	1.451 (11)	1.459 (24)
M-Cl	2.421 (2)	2.285 (5)	C(7)-C(8)	1.394 (12)	1.381 (21)
M-Cl(2)		2.289 (5)	C(8)-C(9)	1.398 (11)	1.416 (24)
M-N(1)	2.103 (5)	2.160 (2)	C(8)-C(11)	1.510 (9)	1.498 (23)
M-C(11)	1.981 (8)		C(9)-C(10)	1.425 (9)	1.425 (20)
M-H		2.6 (1)	P(1)-C(111)	1.822 (7)	1.818 (21)
O(1)-C(11)	1.200 (9)	1.236 (23)	P(1)-C(121)	1.828 (8)	1.799 (24)
N(1)-C(2)	1.322 (11)	1.289 (21)	P(1)-C(131)	1.841 (7)	1.812 (22)
N(1)-C(9)	1.371 (10)	1.386 (19)	P(2)-C(112)	1.845 (8)	
C(2)-C(3)	1.430 (12)	1.396 (23)	P(2)-C(122)	1.807 (9)	
C(3)-C(4)	1.349 (14)	1.298 (25)	P(2)-C(132)	1.825 (9)	
C(4)-C(10)	1.389 (13)	1.421 (25)	$C-C_{av}$[a,b]	1.40 (1)	1.53 (1)
C(5)-C(6)	1.359 (14)	1.275 (32)	C-H		0.9 (2)
C(5)-C(10)	1.445 (13)	1.430 (22)			
			Bond Angles		
Cl(1)-M-Cl(2)		177.0 (1)	N(1)-C(9)-C(10)	120.8 (5)	119.2 (1.1)
P(1)-M-N(1)	173.1 (2)	171.3 (4)	C(7)-C(8)-C(9)	119.6 (5)	121.5 (1.1)
Cl(1)-M-P(1)	96.3 (1)	88.4 (2)	C(7)-C(8)-C(11)	123.2 (5)	114.6 (1.3)
Cl(1)-M-N(1)	90.6 (2)	88.4 (4)	C(9)-C(8)-C(11)	117.2 (5)	123.7 (1.0)
Cl(1)-M-C(11)	170.7 (2)		M-P(1)-C(111)	117.1 (2)	110.6 (5)
Cl(2)-M-P(1)		94.6 (2)	M-P(1)-C(121)	108.9 (2)	115.5 (6)
Cl(2)-M-N(1)		88.5 (4)	M-P(1)-C(131)	116.3 (2)	112.9 (6)
P(1)-M-C(11)	90.1 (2)		C(111)-P(1)-C(121)	106.9 (3)	106.7 (9)
N(1)-M-C(11)	83.1 (2)		C(111)-P(1)-C(131)	101.4 (3)	101.9 (9)
M-C(11)-O(1)	129.5 (3)		C(121)-P(1)-C(131)	105.3 (3)	108.0 (9)
M-C(11)-C(8)	110.6 (4)		C(112)-P(2)-C(122)	101.2 (4)	
M-N(1)-C(2)	128.4 (3)	111.2 (9)	C(112)-P(2)-C(132)	103.4 (3)	
M-N(1)-C(9)	112.1 (4)	126.4 (7)	C(122)-P(2)-C(132)	101.8 (3)	
O(1)-C(11)-C(8)	119.5 (5)	122.3 (1.1)	M-H-C(11)		123 (4)
C(2)-N(1)-C(9)	119.5 (5)	121.4 (1.0)	C(8)-C(11)-H		117 (4)
N(1)-C(9)-C(8)	116.9 (5)	123.5 (9)	O(1)-C(11)-H		120 (4)
			Ring Bond Angles[c]		
CP(1)-Ph(1)	88.0		CP(2)-Ph(1)	65.6	
CP(1)-Ph(2)	33.9		CP(2)-Ph(2)	55.5	
CP(1)-Ph(3)	50.1		CP(2)-Ph(3)	51.1	
			Torsion Angles		
N(1)-M-P(1)-C(121)	82.0 (1.0)	-110.7 (1.8)	C(9)-C(8)-C(11)-O(1)		170.8 (2.3)
N(1)-M-P(1)-C(111)	39.3 (1.0)	10.7 (2.0)	M-P(1)-C(111)-C(211)	-173.0 (1.1)	-52.6 (1.4)
N(1)-M-P(1)-C(131)	159.4 (1.0)	124.3 (2.1)	M-P(1)-C(121)-C(221)	-60.8 (1.1)	-176.4 (1.8)
C(2)-N(1)-C(9)-C(8)		173.1 (2.3)	M-P(1)-C(131)-C(231)	130.2 (1.3)	62.7 (1.4)
N(1)-C(9)-C(8)-C(11)		-9.6 (2.1)			

[a] Average values. Standard deviation from the formula $\sigma = [\sum_i (x_i - \bar{x})^2/n - 1]^{1/2}$. [b] Refers to the C-C bond lengths of the phosphines (phenyl in **3** ethyl in **2a**). [c] Angle between the plane defined by the C(1) (*ipso*-carbon) of each ring and those of the individual phenyl rings.

metal center. The observed H(11)-Pt separation of 2.6 (1) Å is within the accepted range[26,27] for a weak interaction and (within $\pm 3\sigma$) is in agreement with our estimation of 2.35 Å, calculated by assuming sp^2 carbon hybridization at C(11) and a C-H bond length of 1.08 Å (a typical value from neutron diffraction studies). We note that the metal is raised slightly out of the coordination plane, or to put it differently, the ligands appear to retreat slightly relative to the presumed position of the C-H vector.

Comment. Our results with **2a-i**, combined with those previously described,[7] suggest that our $J\{Pt,H(11)\}$ coupling constant is a characteristic of this system and may be attributed to the presence of a three-center interaction of type A. We choose to

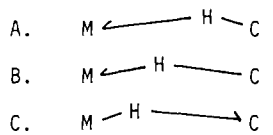

distinguish A from an "agostic" interaction,[26] which we feel to be closer to B. We make this distinction primarily on the basis of our NMR data since neither of the criteria normally associated with an agostic hydrogen—a high-field ^1H shift and substantially reduced $^1J(^{13}C,^1H)$ value—are observed in our complexes. Our previous involvement[28] with bridging hydrides of the type $L_nPt-H-PtL_m^+$, has shown that $^1J(Pt,H)$ in such a molecule can range from 300 to 600 Hz. For a terminal hydride, $^1J(Pt,H)$ is larger. If we accept such a dimeric molecule as a model[34] for our molecules **2**, then a platinum-proton coupling of ca. 20 Hz is less than 10% of a typical bridging situation, once again supporting our assignment of a type A interaction.

It is interesting to speculate as to why the structural unit A has not been observed previously. We feel this stems from (a) the fact that Pt(II) is not very nucleophilic and far less inclined to activate a C-H bond (at room temperature) than other metals in lower oxidatation states and (b) the fortuitously large magnetic moment of ^{195}Pt, which allows the observation of coupling constants which are 50 times smaller than a routine terminal $^1J(^{195}Pt,^1H)$ value. This might not readily be the case for either ^{103}Rh or ^{183}W unless a special effort were made to detect such an interaction. It might be interesting to seek an example of structural type C.

(26) Brookhart, M.; Green, M. L. H. *J. Organomet. Chem.* **1983**, *250*, 395.
(27) Crabtree, R. H.; Holt, E. M.; Lavin, H.; Morehouse, S. *Inorg. Chem.* **1985**, *24*, 1986.
(28) Bachechi, F.; Bracher, G.; Grove, D. M.; Kellenberger, B.; Pregosin, P. S.; Venanzi, L. M. *Inorg. Chem.* **1983**, *22*, 1031.

Table IV. Experimental Data for the X-ray Diffraction Studies[a]

	3	2a
formula	$PdClP_2NOC_{46}H_{36}$	$PtCl_2PNOC_{16}H_{22}$
M_r	822.60	541.33
diffractometer used	PW 1100	CAD 4-F
cryst dimens, mm	0.1 × 0.2 × 0.2	0.15 × 0.22 × 0.20
space group	$P2_1/c$	$P2_1/c$
a, Å	10.159 (4)	14.411 (3)
b, Å	18.262 (5)	9.172 (2)
c, Å	21.171 (5)	15.271 (4)
β, deg	103.27 (3)	107.06 (2)
V, Å^3	3822.8	1929.5 (3)
Z	4	4
ρ(calcd), g cm^{-3}	1.429	1.863
radiation	e	e
measd reflcns	$\pm h,+k,+l$	$\pm h,+k,+l$
μ, cm^{-1}	6.7	77.5
2θ range, deg	$5.0 \leq 2 \leq 48.0$	$5.0 \leq 2 \leq 50.0$
scan type	$\omega/2\theta$	$\omega/2\theta$
scan speed, deg min^{-1}	2.40[b]	10.5 (max speed)
scan width, deg	1.20[b]	1.0 + 0.35 tan θ
max counting time, s	30[b]	40
prescan rejectn limit		0.5 (2σ)
prescan accept limit		0.03 (33σ)
bkgd time, s	14	0.5 × scan time
horiz receiving aperture	1.0°	[2.0 × tan θ] mm
vert receiving aperture	0.6°	4.0 nm
no. of indept data collcd	5980	3367
no. of obsd data [$I \geq 3\sigma(I)$]	3721	2362
R[c]	0.058	0.045
R_w[d]	0.064	0.051

[a] Collected at room temperature. [b] Parameter kept constant over the range during the data collection. [c] $R = \sum(|F_o| - |F_c|)/\sum|F_o|$. [d] $R_w = [\sum w(|F_o| - |F_c|)^2/\sum wF_o^2]^{1/2}$. [e] Mo K$\bar{\alpha}$ graphite monochromated; λ = 0.710 69 Å.

Experimental Section

Crystallography. Crystals suitable for X-ray diffraction of compound **2a**, light yellow in color and air stable, were obtained by slow evaporation from a CH_2Cl_2/hexane solution; for compound **3**, air-stable, yellow crystals were obtained by slow evaporation from a chloroform solution. Data were collected on automatic diffractometers by using the parameters listed in Table IV: a variable scan speed was used to obtain a constant statistical precision on the collected intensities for compound **2a**, while constant data collection parameters (scan speed, scan width, background time) were used for compound **3**. Data were corrected for Lorentz and polarization factors[29] and absorption with the data reduction programs of the CAD4-SDP package[30a] for **2a** or were corrected as described elsewhere[30b] for **3**. The standard deviations on intensities were calculated in terms of statistics alone, and intensities were considered as observed if $I_{net} \geq 3\sigma(I_{tot})$. The structures were solved by a combination of Patterson and Fourier methods and refined by block-diagonal least-squares methods[30b] using a Cruckshank[31] weighting scheme. The function minimized was $[\sum w(F_o) - 1/k(F_c)]^2$. Scattering factors were taken from ref 32, and the contribution of the anomalous dispersion[32] for Pd, Cl, P, and O atoms was taken into account. No extinction correction was found to be necessary on either set of data.

Structural Study of $PtCl_2(C(O)C_9H_7N)(PEt_3)$ (2a). A light yellow crystal of prismatic shape was mounted on a glass fiber for the data collection with a CAD4 diffractometer. From the systematic absences the space group was assigned to be $P2_1/c$. Cell constants were obtained by a least-squares fit of the 2θ values of 25 high-angle reflections ($11.5 \leq \theta \leq 14.0$) made by using the CAD4 centering routines.[27a] Crystallographic ($11.5 \geq \theta \geq 14.0$) made by using the CAD4 centering routines.[27a] Crystallographic data and relevant parameters for the data collection are listed in Table IV. Three standard reflections ($3\bar{3}1$, $2\bar{2}5$, $4\bar{1}4$) were used to check the stability of the crystal and the experimental conditions; no significant variation was detected. The orientation of the crystal was checked by measuring three reflections ($1\bar{3}3$, $4\bar{1}1$, $4\bar{1}4$) every 300. An empirical absorption correction was applied by using the azimuthal scans of three reflections with high χ angles ($\chi > 83°$): 312, 412, 514. Transmission factors were in the range 0.80–0.99. The structure was refined by block-diagonal least-squares methods as described above with anisotropic temperature factors used for all atoms. Upon convergence a Fourier difference map revealed some of the hydrogens of the ligands, and in particular that bound to C(11), and this was included in the refined model, leading to a satisfactory convergence (C–H = 0.9 (1) Å and Pt–H = 2.6 (1) Å; see Table III and Table V). During the refinement, the contribution of the other hydrogen atoms, held fixed in their idealized calculated positions, was taken into account (C–H = 0.98 Å; B_{iso} = 7.50 Å^2 for the H atoms of the phosphine, and for the other H atoms a B_{iso} higher than the B_{eq} of the bound atom by 1.5 Å^2 was used). Final positional parameters are listed in Table V. Selected bond distances and angles are given in Table III. An ORTEP[33] view of the molecule is given in Figure 2. Tables of coordinates and thermal factors (Table S1), an extended list of bond lengths and angles (Table S2), and

Table V. Final Positional Coordinates for **3** (Esd's in Parentheses)

	x/a	y/b	z/c
Pd	0.791 92 (5)	0.114 11 (3)	0.078 18 (2)
P(1)	0.935 84 (17)	0.103 32 (10)	0.176 89 (8)
P(2)	0.568 18 (22)	0.323 14 (11)	0.089 04 (10)
Cl(1)	0.961 92 (20)	0.146 16 (14)	0.019 42 (10)
N	0.639 72 (56)	0.121 44 (32)	−0.007 72 (26)
C(2)	0.651 24 (85)	0.141 92 (47)	−0.066 12 (41)
C(3)	0.537 92 (98)	0.141 56 (55)	−0.120 54 (47)
C(4)	0.415 43 (93)	0.121 41 (52)	−0.112 05 (45)
C(5)	0.274 54 (92)	0.076 70 (53)	−0.036 19 (45)
C(6)	0.270 33 (90)	0.055 57 (49)	0.024 89 (43)
C(7)	0.387 46 (85)	0.055 60 (47)	0.076 20 (41)
C(8)	0.510 61 (71)	0.077 33 (40)	0.063 78 (34)
C(9)	0.515 98 (70)	0.100 07 (38)	0.001 35 (34)
C(10)	0.400 02 (78)	0.099 34 (42)	−0.051 36 (38)
C(11)	0.642 03 (68)	0.076 45 (38)	0.114 60 (33)
O(1)	0.645 85 (56)	0.048 42 (31)	0.166 27 (27)
C(111)	0.880 59 (67)	0.141 53 (37)	0.246 34 (32)
C(211)	0.958 13 (74)	0.129 53 (41)	0.309 41 (35)
C(311)	0.917 34 (87)	0.157 23 (50)	0.363 35 (42)
C(411)	0.798 54 (85)	0.197 32 (47)	0.354 16 (41)
C(511)	0.721 02 (84)	0.211 57 (47)	0.291 93 (41)
C(611)	0.764 15 (74)	0.184 25 (41)	0.238 06 (35)
C(121)	0.970 71 (68)	0.006 62 (38)	0.194 16 (32)
C(221)	1.031 34 (76)	−0.032 02 (42)	0.151 68 (36)
C(321)	1.054 29 (92))	−0.107 92 (53)	0.160 45 (45)
C(421)	1.018 92 (93)	−0.144 08 (52)	0.212 08 (45)
C(521)	0.954 97 (101)	−0.106 13 (57)	0.252 83 (49)
C(621)	0.932 91 (86)	−0.028 74 (48)	0.244 84 (41)
C(131)	1.102 82 (68)	0.146 62 (38)	0.186 01 (33)
C(231)	1.223 96 (71)	0.109 39 (42)	0.212 06 (34)
C(331)	1.347 55 (86)	0.145 63 (49)	0.215 97 (42)
C(431)	1.347 31 (88)	0.218 39 (49)	0.196 11 (42)
C(531)	1.228 11 (89)	0.255 66 (51)	0.170 69 (44)
C(631)	1.103 45 (81)	0.218 46 (45)	0.165 81 (39)
C(112)	0.456 57 (82)	0.315 08 (46)	0.007 26 (40)
C(212)	0.487 90 (97)	0.349 13 (55)	−0.046 27 (47)
C(312)	0.397 83 (113)	0.341 75 (64)	−0.108 47 (55)
C(412)	0.279 98 (112)	0.301 17 (61)	−0.113 09 (54)
C(512)	0.250 46(105)	0.267 70 (59)	−0.059 47 (51)
C(612)	0.338 24 (92)	0.274 88 (51)	0.001 01 (44)
C(122)	0.486 64 (79)	0.396 29 (44)	0.123 16 (38)
C(222)	0.527 77 (95)	0.407 66 (52)	0.190 61 (46)
C(322)	0.472 11 (99)	0.464 61 (56)	0.221 71 (48)
C(422)	0.371 91 (99)	0.509 10 (55)	0.183 69 (47)
C(522)	0.327 95 (93)	0.499 29 (52)	0.116 61 (44)
C(622)	0.385 79 (86)	0.441 96 (48)	0.087 94 (42)
C(132)	0.717 64 (79)	0.369 21 (42)	0.074 19 (37)
C(232)	0.815 10 (94)	0.323 79 (53)	0.056 59 (46)
C(332)	0.936 34 (105)	0.353 93 (59)	0.045 21 (50)
C(432)	0.957 67 (106)	0.426 96 (59)	0.053 76 (52)
C(532)	0.863 19 (106)	0.473 27 (58)	0.069 38 (51)
C(632)	0.741 25 (97)	0.443 21 (50)	0.080 25 (42)

(29) Arndt, V. V.; Willis, B. T. M. *Single Crystal Diffractometry*; Cambridge University Press: New York, 1966; p 286.
(30) (a) *Enraf-Nonius Structure Determination Package (SDP)*; Enraf-Nonius: Delft, Holland, 1980. (b) For the data collection and references to least squares, structure factors and Fourier programs see: Albinati, A.; Brückner, S. *Acta Crystallogr., Sect. B: Struct. Crystallogr. Cryst. Chem.* **1978**, *B34*, 3390.
(31) Cruickshank, D. W. J. In *Computing Methods in Crystallography*; Ahmed, A., Ed.; Munksgaard: Copenhagen.
(32) *International Tables for X-ray Crystallography*; Kynoch: Birmingham, 1976; Vol. 4
(33) Johnson, C. K. *Oak Ridge Natl. Lab.* [Rep.], *ORNL* (U. S.) **1965**, ORNL-3794.
(34) The model is certainly inadequate; however, we know of none better.

Table VI. Final Positional Coordinates for **2a** (Esd's in Parentheses)

	x/a	*y/b*	*z/c*
Pt	0.22427 (4)	0.21215 (7)	0.08800 (4)
P(1)	0.1391 (3)	0.2474 (5)	-0.0573 (3)
Cl(1)	0.3624 (3)	0.2518 (6)	0.0472 (3)
Cl(2)	0.0909 (3)	0.1696 (7)	0.1367 (3)
N(1)	0.3145 (10)	0.1476 (15)	0.2220 (8)
C(2)	0.3092 (12)	0.0091 (18)	0.2341 (12)
C(3)	0.3798 (14)	-0.0590 (22)	0.3050 (13)
C(4)	0.4532 (13)	0.0098 (20)	0.3591 (12)
C(5)	0.5332 (12)	0.2508 (24)	0.4123 (11)
C(6)	0.5359 (13)	0.3889 (26)	0.4043 (12)
C(7)	0.4601 (12)	0.4670 (27)	0.3357 (12)
C(8)	0.3858 (10)	0.3870 (19)	0.2780 (10)
C(9)	0.3835 (11)	0.2329 (17)	0.2828 (10)
C(10)	0.4586 (11)	0.1639 (18)	0.3527 (10)
C(11)	0.3062 (15)	0.4765 (22)	0.2163 (12)
O(1)	0.3150 (12)	0.6086 (14)	0.2048 (12)
C(111)	0.1751 (13)	0.1180 (22)	-0.1314 (12)
C(211)	0.1723 (15)	-0.0422 (24)	-0.1010 (14)
C(121)	0.0096 (16)	0.2319 (25)	-0.0819 (15)
C(221)	-0.0533 (18)	-0.2637 (28)	-0.1789 (17)
C(131)	0.1653 (15)	0.4204 (23)	-0.1022 (13)
C(231)	0.1392 (20)	0.5514 (34)	-0.0529 (19)
H(C11)	0.2499 (82)	0.4344 (99)	0.1941 (77)

a table of structure factors (Table S3) are given in the supplementary material.

Structural Study of $\overline{PdCl(C(O)C_9H_6N)PPh_3}\cdot PPh_3$ (3). A suitable crystal of prismatic habit was chosen for the data collection and mounted at a random orientation on a glass fiber. Crystal data and data collection parameters are listed in Table IV. The determination of the cell constants, space group, and data collection were carried out, at room temperature, on a Philips PW1100 four-circle diffractometer. From systematic absences the $P2_1/c$ space group was assigned. The cell parameters were obtained by least-squares fit of the 2θ values of 25 accurately centered, high-order reflections ($16.0 \leq 30.0°$). Three standard reflections ($\bar{2}34$, $2\bar{3}\bar{4}$, $1\bar{3}4$) were measured every 180 min to check the stability and orientation of the crystal. No significant variations were detected. Anisotropic temperature factors for Pd, P, and Cl atoms were used during the refinement. After the localization and partial refinement of the Pd-containing moiety, additional peaks in the Fourier difference map revealed the presence of an additional clathrated phosphine molecule in the cell. The hydrogen of the carbon atoms were placed in idealized positions (C-H bond length = 0.95 Å, B_{iso} = 5.5 Å^2, and their contribution was taken into account but not refined. An ORTEP view (with ellipsoids scaled at 30% probability) is given in Figure 1. The final positional parameters are given in Table VI. Selected bond distances and angles are given in Table III. Tables of coordinates and thermal factors (Table S4), and extended list of bond lengths and angles (Table S5), and a stable of structure factors (Table S6) are given in the supplementary material.

NMR spectra were measured as $CDCl_3$ solutions on Bruker HX-90 and WM-250 spectrometers, with the *former to be recommended* due to problems associated with ^{195}Pt relaxation.[7] Chemical shifts are ±0.01 ppm; coupling constants are ±0.5 Hz.

The complexes **2** were available in ≥90% yield by reaction of **1** with 0.5 equiv of the dimer in CH_2Cl_2 or $CHCl_3$. Recrystallization from CH_2Cl_2/hexane gave analytically pure complex.

The acyl complexes are prepared by refluxing a $CHCl_3$ solution of **2** for 12 h. Removal of the solvent gives the crude product, which can be recrystallized from CH_2Cl_2/hexane. $\overline{PdCl(C(O)C_9H_6N)(PPh_3)}\cdot PPh_3$ was prepared by cleavage of the dimer $[PdCl(C(O)C_9H_6N)]_2$[4] with 2 equiv of PPh_3. See Table I for analytical data.

Acknowledgment. We thank the ETH Zürich and the Swiss National Science Foundation for support and the Johnson-Matthey Research Centre, England, for the loan of precious metals. A.A. acknowledges partial support from the MPI and helpful discussions with Dr. De Martin.

Supplementary Material Available: Tables for coordinates and thermal factors (Tables S1 and S4) and extended lists of bond lengths and bond angles (Tables S2 and S5) (16 pages); tables of structure factors (Tables S3 and S6) (34 pages). Ordering information is given on any current masthead page.

Contribution from the Institute of Pharmaceutical Chemistry, University of Milan, I-20131 Milan, Italy, and Inorganic Chemistry Laboratory, ETH, CH-8982 Zürich, Switzerland

^nJ(Pt,H) and Pt←H-C Interactions in Schiff Base Complexes of 2-(Benzylideneamino)-3-methylpyridine. Molecular Structures of Dichloro(2-((2,4,6-trimethylbenzylidene)amino)-3-methylpyridine)(triethylarsine)platinum(II) and Dichloro(2-amino-3-methylpyridine)(triethylphosphine)palladium(II)

A. Albinati,*† C. Arz,‡ and P. S. Pregosin*‡

Received July 22, 1986

The preparation and characterization of the complexes *trans*-$PtCl_2$ {2-(N=CHR)-3-$CH_3C_5H_3N$}($AsEt_3$) and *trans*-$PdCl_2${2-(N=CHR)-3-$CH_3C_5H_3N$}(PEt_3) (R = a substituted aryl group) are reported. The molecular structures of *trans*-$PtCl_2${2-(N=CH(mesityl))-3-methylpyridine}($AsEt_3$) and *trans*-$PdCl_2$(2-amino-3-methylpyridine)(PEt_3) have been determined by X-ray analysis. The former reveals a relatively short imine proton-platinum separation of 2.43 (8) Å, which is confirmed in solution by the observation of a proton-platinum coupling constant. Despite this spin-spin coupling and the proximity of the proton to the metal, this interaction is considered to be weak. Crystal data for the Pt complex are as follows: a = 8.177 (2) Å, b = 10.832 (1) Å, c = 14.370 (2) Å; α = 82.99 (2)°, β = 81.29 (2)°, γ = 89.41 (2)°; V = 1248.7 (8) Å^3; space group = $P\bar{1}$, Z = 2. Crystal data for the Pd complex are as follows: a = 13.866 (1) Å, b = 7.597 (1) Å, c = 16.555 (1) Å; β = 101.971°; V = 1705.96 (6) Å^3; space group = Cc, Z = 4. ^1H, ^{13}C, and ^{31}P NMR data are reported for the complexes.

Introduction

There is a long-standing interest in the interaction of transition metals with proximate carbon-hydrogen bonds.[1]

Molecular structure studies suggest M←H-C bonding interactions occur at distances of ca. 1.8-2.2 Å,[2,3] and in solution there are an increasing number of molecules in which the hydrogen of a C-H bond develops some hydride-like character.[4] This latter category of complexes is conventionally said to display an "agostic" covalent interaction,[2] which can be thought of as a two-electron three-center bond. In solution the agostic M←H-C system is

†University of Milan.
‡ETH.

(1) Shilov, A. E. *Activation of Saturated Hydrocarbons by Transition Metal Complexes*; D. Reidel: Dordrecht, Holland, 1984.
(2) Brookhart, M.; Green, M. L. H. *J. Organomet. Chem.* **1983**, *250*, 395.
(3) Crabtree, R. H.; Holt, E. M.; Lavan, M.; Morehouse, S. M. *Inorg. Chem.* **1985**, *24*, 1986.
(4) Bennett, M. A.; McMahon, I. J.; Pelling, S.; Robertson, G. B.; Wickramasinghe, W. A. *Organometallics* **1985**, *4*, 754. Ittel, S. D.; Van-Catledge, F. A.; Jesson, J. P. *J. Am. Chem. Soc.* **1979**, *101*, 6905. Calvert, R. B.; Shapley, J. R. *J. Am. Chem. Soc.* **1978**, *199*, 7726.

0020-1669/87/1326-0508$01.50/0